Improving Regenerative Energy Receptivity in Metro Transit Systems
Coordinated Train Control Algorithm

Haichuan Tang, C. Tyler Dick, and Xiaoyun Feng

Algorithms for current automatic train operation (ATO) focus mainly on reducing the mechanical energy of motion for a single train within an existing timetable. However, the reuse of regenerative energy is another factor that contributes to energy consumption and conservation in multi-train networks. To improve regenerative energy receptivity and energy savings in a bidirectional metro transit network, this study formulated a coordinated train control algorithm that was based on genetic algorithm techniques. The energy saving potential of different station departure time intervals between two opposing trains (synchronization time) was tested. Simulation on the Visual C++ platform demonstrated that the algorithm could provide an optimal train speed profile with better energy performance while also satisfying operational constraints. Different synchronization times have different optimization ratios. This research was another step to facilitate the development of an ATO control algorithm that considers overall energy consumption. Increased knowledge of the influence of synchronization time at stations on energy consumption in regenerative multitrain networks will also aid in the design of more energy-efficient timetables.

Regenerative braking is a braking mechanism that decelerates the vehicle by converting its kinetic energy into electric energy. Regenerative braking has been widely applied on electric trains, particularly in metro transit systems. Compared with trains with only pneumatic braking, studies show that the use of regenerative braking on metro trains can provide energy savings of 10% to 45%, depending on system characteristics (*1*). In addition to saving energy, regenerative braking also helps mitigate voltage fluctuation when multiple trains accelerate simultaneously during peak hours.

For maximization of the use of regenerative braking energy, synchronization of acceleration and braking among multiple trains is a key issue because regenerative energy can only be reused when there are power requirements in the same power section. For instance, if one train accelerates while the other train brakes in the same power section, this acceleration can take advantage of the regenerative braking energy. The total energy cost at substations is consequently reduced. Two alternatives are currently used to improve system regenerative receptivity: the use of an energy efficient timetable and optimization of an automatic train operation (ATO) algorithm.

Many researchers have dealt with timetable optimization. In such a problem, dwell time, interstation running time, and service frequency are the principal factors for energy efficient timetable design. Some studies have adjusted dwell time by delaying the departure of trains to synchronize acceleration and braking events. Applied control methods include predictive fuzzy control, search techniques, and heuristics (*2–4*). Evolutionary methods (such as genetic algorithms) have also been used to investigate the influence of running time on operating cost (*5*). Service frequency and dwell time are also regarded as influential parameters to be optimized (*6*). But the application of energy efficient timetables is limited, as service quality is negatively affected as a result.

Another alternative to improve regenerative synchronization is to adjust train speed profiles through the use of an optimized ATO algorithm within a predefined timetable, so that service quality can be maintained. ATO systems are used to generate optimal driving commands for train speed regulation. Traditional ATO algorithms are generally designed to reduce the mechanical energy consumption of single-train operation by altering its train speed profile while still satisfying operational constraints. Through the latest train control technologies, such as communications-based train control (CBTC) systems, a train could be aware of the projected speed profiles of other trains in the same power section before leaving its station (*7*). Accordingly, power flow could be predicted in real-time, allowing for the design of coordinated train control algorithms for ATO systems where acceleration and braking are synchronized with other trains in the same power section.

Traditional ATO algorithms can be achieved with analytical methods (*8, 9*) and numerical methods (*10–12*). On the basis of these methods, recent research has proved the optimality of regenerative receptivity through train speed coordination in single-direction operation; the gradient method and sequential quadratic programming have been introduced (*13–15*). However, for most urban transit systems, the bidirectional application of coordinated control algorithms should also be studied. In addition, for this large-scale, nonlinear problem, a global optimization method should be applied to ensure the effectiveness of the solution.

With the dual objectives of maintaining schedule requirements and optimizing energy efficiency, this study examined the prospects for recovering and reusing energy from regenerative brakes under transit system operating conditions. Assuming that two opposing trains are operated in the same power section, analysis of the dynamic and electric performance of the later-departing train was conducted in accordance with the prescribed speed profile of the earlier-departing train. To obtain the minimum energy cost at the substation level, genetic algorithms (GAs) were applied to search for the optimal speed profile for the later-departing train. For demonstration of an application of

H. Tang and X. Feng, Southwest Jiaotong University, West Section, High-Tech Zone, Chengdu 611756, China; C. T. Dick, Rail Transportation and Engineering Center–RailTEC, Department of Civil and Environmental Engineering, University of Illinois at Urbana–Champaign, 205 North Mathews Avenue, Urbana, IL 61801. Corresponding author: H. Tang, hctang@illinois.edu.

the optimization framework, energy optimization potentials of transit systems with different synchronization times were compared.

ARCHITECTURE OF THE CBTC SYSTEM

The coordinated train control model presented in this paper is based on CBTC systems.

Conventional train control systems are not a suitable platform for coordinated driving strategy design, because of the limitations of track circuit communication. For example, the precision of train location determination largely depends on the length of the track circuit. And only a small quantity of operational information (speed, signal aspect, etc.) can be transmitted to onboard systems through track circuits. Those limitations make it difficult for train control systems to estimate electrical parameters in the network and generate the optimal control strategy.

Unlike track circuit–based communication, CBTC is a train control system that improves safety, efficiency, and traffic management by making use of bidirectional train-to-wayside data communication. The system provides more information for train operation and has been widely applied to light rail, heavy rail, and commuter rail systems in many countries. A typical CBTC system architecture is shown in Figure 1 (*16*).

In the CBTC architecture, the automatic train supervision (ATS) system fills the role of the control center, which is dedicated to train and schedule adherence. For trains in the network, the ATO system provides speed regulation and other functions. Automatic train protection (ATP) prevents trains from collisions or going over speed. Train control and status information are exchanged with other subsystems and trains through the data communication network to ensure the proper functionality of CBTC.

The coordinated train control algorithm proposed by this study was designed for the ATO module. Because of the lack of operational information from neighboring trains, traditional ATO algorithms regulate the train speed profile to reduce mechanical energy consumption from a single train's perspective. However, for CBTC-based ATO subsystems, information on neighboring trains, such as location, speed, and travel direction, can be acquired through a data exchange network. This information allows the ATO subsystem to estimate and predict energy consumption and voltage fluctuation based on the operational status of trains in the same power section. By choosing the proper acceleration and braking commands to

coordinate its speed profile with those of other trains, power peaks can be reduced by absorbing regenerative braking energies.

MODEL DESCRIPTION

Assumptions

The model presented in this paper relies on several key assumptions:

- A CBTC-based ATO subsystem is used for model analysis.
- The electrical network is based on direct current (DC) power supply from substations and no inductive resistance is considered.
- Two opposing trains (one eastbound and one westbound) are running in the same power section.
- The speed and position of the earlier-departing train (eastbound) are known.
- Traction energy is provided by power substations at both ends of the power section.
- Resistance in the catenary is evenly distributed.
- Substations are nonreversible. No wayside energy storage devices are included in this problem.

Electrical Network Model

The electrical network model varies according to the current location and status of the two trains within the same power section. As shown in Figure 2, two trains (U_{dc1} and U_{dc2}) are running between two substations (U_{d0}).

The model follows the common practice in rapid transit systems where three-phase alternating current electricity from the general power supply is converted into DC electricity at a substation that feeds train operation via the catenary (*17, 18*). In this model, the current conversion at the substation is not considered. Thus, the substation can be described by its external voltage-current characteristics as a Thevenin equivalent voltage source U_{d0}. In the model, R_s is an equivalent resistor and I_{u1} and I_{u2} are currents from substations at the ends of the power section.

Two trains are modeled as ideal current sources, I_{S1} and I_{S2}. Their actual power during operation varies according to the current and voltage level. U_{dc1} and U_{dc2} are the catenary voltages of the eastbound train and westbound train, respectively. Since the catenary resistance
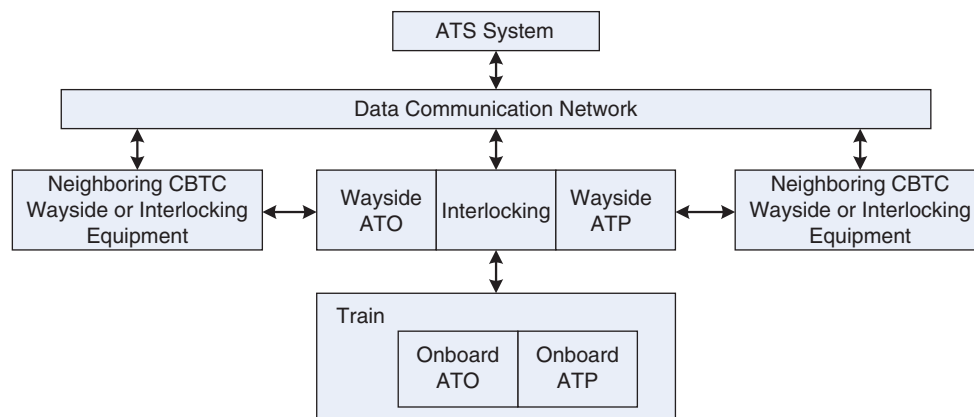
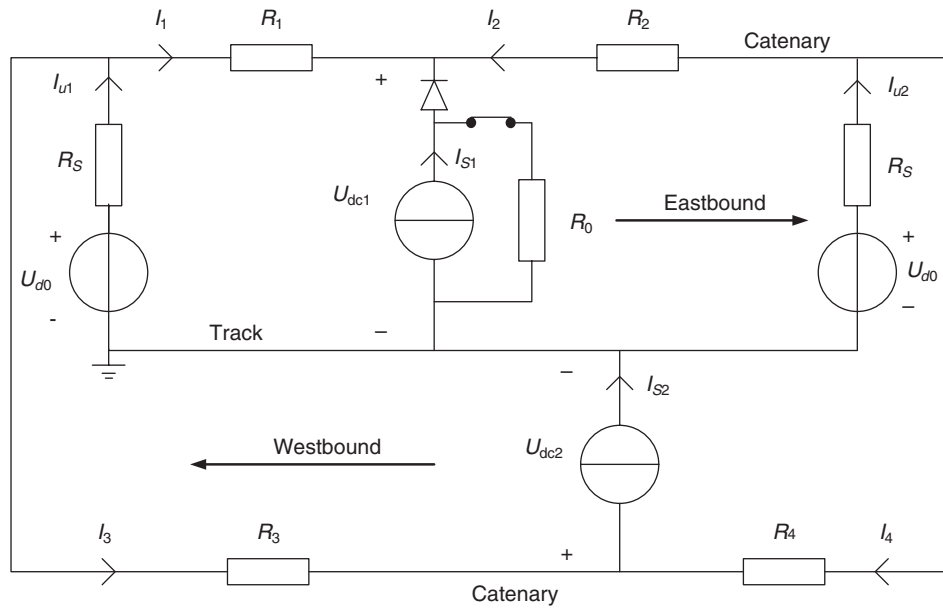

FIGURE 1   Typical CBTC system.

FIGURE 2 Electrical model when the eastbound train (I_{s1}) is in braking status and the westbound train (I_{s2}) is in traction status.

is assumed to be uniform, the values of the four catenary equivalent resistors R_1, R_2, R_3, and R_4 only depend on the current position of trains within the power section. R_0 is an onboard resistor that is applied during dynamic braking when regenerated electricity cannot be used by other trains.

During operation, when both trains are accelerating, they take energy from substations and the currents I_{u1} and I_{u2} are positive. In this state, the required energy will rise sharply when either train starts to accelerate. The required energy will decrease when the maximum speed is reached and less power is required during a cruise state. When the eastbound train approaches the station ahead, it starts to brake. Regenerative braking is applied and the train's motor is converted into a generator. Current I_{S1} is transmitted to the overhead wire and is absorbed by the neighboring train in traction status. When the network is not receptive (regenerative energy cannot be fully absorbed), the excess electricity is dissipated by the resistor R_0 onboard the eastbound train as in dynamic braking. The diode in the electrical network representation of this train is used to restrict the direction of current during dynamic braking. In practice, dynamic braking is not encouraged, as it wastes energy and also presents a potential risk of overheating and fire. Thus, dynamic braking is not considered as rewarding as regenerative braking.

Mathematical Model

The study aimed to find the optimal speed profile for the westbound train, according to the prescribed movement of the eastbound train, to minimize the total energy consumption as measured at the substations.

The model variables are defined as follows:

s_1, s_2 = travel distance of eastbound train and westbound train, respectively;
v_1, v_2 = speed of eastbound train and westbound train, respectively;

$v_{\text{limit}}(s)$ = speed restriction at position s;
P_1, P_2 = electrical power of eastbound train and westbound train, respectively;
n_{2T} = coefficients of applied tractive effort for westbound train;
n_{2B} = coefficients of applied braking effort for westbound train;
$F_{\text{max2}}(U, v)$ = maximum tractive effort applied on westbound train for voltage U, at speed v;
$B_{\text{max2}}(U, v)$ = maximum braking effort applied on westbound train for voltage U, at speed v;
$R_{\text{air}}(v)$ = train resistance;
$R_G(s)$ = gradient resistance;
$R_C(s)$ = curvature resistance;
Δr = equivalent resistance of the catenary per unit length;
μ_t = efficiency of driver system in tractive state;
μ_g = efficiency of driver system in braking state;
S = required interstation distance;
T = required interstation running time;
ΔT_{depart} = synchronization time between two train departures from opposite stations;
M = train weight; and
J = total energy cost at substations.

In the definition of F_{max2}, B_{max2}, maximum effort means tractive or braking effort when the driver's handle is at full level. These values are influenced by how much power can be provided by the power section (U_{dc}). The values also vary with train speed (v).

On the basis of the network description in the previous section, the total energy cost for the power section at the substations can be written as

$$\min J = \int_0^T (U_{d0} \cdot I_{u1} + U_{d0} \cdot I_{u2})\, dt \tag{1}$$

where t is train running time.

Four types of constraints are mainly considered in this model: infrastructure, motion equations, electrical constraints, and operational constraints. Each will be described in the following sections.

Infrastructure

Line profile (gradient) and alignment (curvature) are very influential on train performance and energy consumption. These two infrastructure factors are measured at each location by gradient slope and curvature angle, respectively. The resultant grade and curvature resistance forces experienced by a train are described in the motion equations in the next section.

Another infrastructure constraint is the maximum allowable speed, which is generally determined by curvature, turnouts, or other operational conditions. Speed restrictions are related to mileposts along the route, and the speed of the westbound train at location s_2 must obey these limits:

$$0 \le v_2(s_2) \le v_{\text{limit}}(s_2) \tag{2}$$

Motion Equations

The motion equation for this problem was established on the basis of a point-mass model of the train. This is a reasonable assumption, given that the length of most transit trains is relative to the rate of change of alignment and profile geometry. When the train is in the traction state, it is experiencing tractive effort, train resistance, grade resistance, and curve resistance. When in the regenerative braking state, regenerative effort will be applied instead of tractive effort. The expression is shown below:

$$\frac{ds_2}{dt} = v_2 \tag{3}$$

$$M \cdot v_2 = \begin{cases} n_{2T}F_{\max 2}(U_{\text{dc}2}, v_2) - R_{\text{air}}(v_2) - R_G(s_2) - R_C(s_2) \\ n_{2T}B_{\max 2}(U_{\text{dc}2}, v_2) - R_{\text{air}}(v_2) - R_G(s_2) - R_C(s_2) \end{cases} \tag{4}$$

where the tractive and braking coefficients n_{2T} and n_{2B} satisfy

$$\begin{cases} n_{2T} \in [0,1] & \text{(traction)} \\ n_{2B} \in [-1,0) & \text{(braking)} \end{cases} \tag{5}$$

Electrical Constraints

According to Kirchhoff's circuit law, the DC circuit power networks in this optimal control problem are modeled via equality constraints as

$$\begin{bmatrix} U_{\text{dc}2} \\ U_{\text{dc}1} \\ I_{u1} \\ I_{u2} \end{bmatrix} = \begin{bmatrix} G_{11} & G_{12} & G_{13} & G_{14} \\ G_{21} & G_{22} & G_{23} & G_{24} \\ G_{31} & G_{32} & G_{33} & G_{34} \\ G_{41} & G_{42} & G_{43} & G_{44} \end{bmatrix} \begin{bmatrix} U_{d0} \\ U_{d0} \\ I_{S2} \\ I_{S1} \end{bmatrix} \tag{6}$$

where G_{ij} $(i, j = 1, 2, 3, 4)$ are elements of the conductance matrix.

As the internal resistance of the catenary is assumed to be uniform, the equivalent resistances R_1, R_2, R_3, and R_4 in Figure 2 are defined by the positions of the trains in the power section:

$$R_1 = s_1 \cdot \Delta r$$
$$R_2 = (S - s_1) \cdot \Delta r$$
$$R_3 = (S - s_2) \cdot \Delta r$$
$$R_4 = s_2 \cdot \Delta r \tag{7}$$

Train power is calculated in real-time according to the force coefficient, actual train speed, and the catenary voltage. The westbound train's power demands during traction and braking are given in Equation 8.

$$P_2 = \begin{cases} n_{2T} \cdot F_{\max 2}(U_{\text{dc}2}, v_2) \cdot v_2 \cdot \mu_t \\ \dfrac{n_{2B} \cdot B_{\max 2}(U_{\text{dc}2}, v_2) \cdot v_2}{\mu_g} \end{cases} \tag{8}$$

Operational Constraints

Adhering to the operating schedule is essential for urban transit systems. All optimized speed profiles must respect interstation time and distance requirements. Considering a section between two stations, each train departs from one station and stops at the other. These operational constraints can be described by

$$v_{1,2}(0) = 0 \qquad v_{1,2}(T) = 0$$
$$s_{1,2}(0) = 0 \qquad s_{1,2}(T) = S \tag{9}$$

As two running directions have been considered in the same section, a departure constraint is also required for operation issues:

$$t_2(0) - t_1(0) = \Delta T_{\text{depart}} \tag{10}$$

Equation 10 defines synchronization time, which is the station departure time interval for two opposing trains. This constraint ensures that within the interstation section, the westbound train leaves the station ΔT_{depart} seconds later than the eastbound train.

APPLICATION OF ENHANCED GAs

A GA is a global search algorithm technique based on the principle of natural selection. The algorithm mimics the evolution of biological organisms to achieve optimal solutions with a given objective function in an artificial system.

Compared with other optimization techniques, the GA has several advantages for large-scale optimization problems. Because this is a large-scale, nonlinear problem, the GA was proposed to solve the coordinated train control problem to ensure the solution's effectiveness and efficiency.

Problem Coding

In this problem, the control variable is the coefficient of the applied force, which is defined as the percentage of maximum traction or
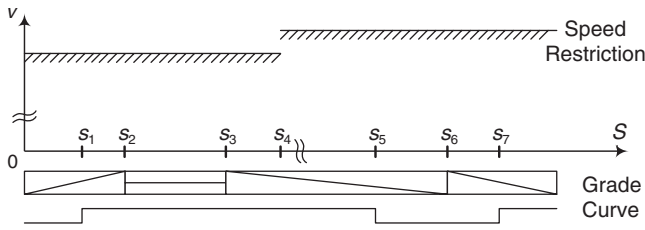
FIGURE 3   Control switching points along the line.

braking force applied by the train. The force was discretized in 10% increments as 0, ±0.1, ±0.2, . . . , ±0.9, ±1. The plus sign represents traction, while the minus sign represents braking. Coasting is represented by 0. During train operation, the control variable can be changed according to different infrastructure parameters, such as speed restriction, gradient, or curvature. Thus, the solution can be modeled as a sequence of control variables at specific control switching points.

An example of a control switching point is illustrated in Figure 3. Control switching points s_1 to s_7 are based on infrastructure parameters.

A chromosome is a possible sequence of the control variable (for example: [n_{21}, n_{22}, n_{23}, n_{24}, n_{25}, n_{26}, n_{27}]). Each gene (n_{2i}) represents the coefficient of the applied force at corresponding position s_i. The n_{2i} value can be any discretized number from −1 to +1.

As the number of control switching points is predetermined, the length of the chromosome is fixed.

Fitness Function

The objective of this algorithm is to minimize system electrical energy consumption with the restriction of travel time and distance. However, the GA is formulated to find a maximum value during the search process, as fitness values are always positive. In addition, as a multi-criterion optimization, a proper combination form needs to be determined to satisfy the operational constraints. Several modifications have been made to the traditional GA to deal with the above issues.

Therefore, the fitness function has been formulated in Equation 11.

$$f = \frac{1}{\left(\sum \left(U_{d0} \cdot \Delta I_1 + U_{d0} \cdot \Delta I_3 \right) + w_S \cdot \left| s_2(T) - S \right| + w_V \cdot \left| v_2(T) - 0 \right| \right)} \tag{11}$$

The first term is the minimization objective for network energy consumption. The following two terms ensure the punctuality and stop accuracy for the train arriving at the next station, where w_s and w_v are weights for travel distance and speed, respectively. These last two terms have higher weights to ensure that the operational requirements are satisfied first.

The reversed formulation ensures the minimum energy consumption can be achieved when the maximum fitness value is found by the GA.

Combinational Selection

Selection is the process used to choose a group of chromosomes from a population for later breeding based on their fitness values.

Individuals with higher fitness values are more likely to be chosen to produce the next generation. Two main selection strategies are applied: roulette wheel selection and rank selection.

Roulette wheel selection is a fitness-proportionate selection method and, because of its efficiency, is commonly used in best individual selection. The probability of a chromosome being selected is proportional to its fitness. However, since this method can quickly eliminate the lower-fitted individuals, the solution may inadvertently converge to a local optimum point.

To avoid this possibility, rank selection is used for population selection in the early stages. Instead of using fitness value, rank selection assigns ranking numbers (from 1 to N) to each chromosome. The worst is rank 1 and the best is rank N. The selection probability is then established according to this ranking number. In this way, less-fitted chromosomes have more chances to survive.

The combination of these two methods ensures a variety of species in the early evolution stage and that multiple good solutions will emerge for breeding. As the evolution proceeds, with the use of roulette wheel selection, better-fitted individuals have greater chances of selection. Therefore, the later evolution process will be accelerated.

Adaptive Crossover

Crossover is the process of taking more than one parent chromosome and producing offspring by exchanging part of their gene information. Crossover has two key parameters: crossover probability and crossover operator. The former decides how likely an individual is to be chosen for crossover operation, while the latter decides how parents exchange information.

To ensure the efficiency of evolution, adaptive probability has been applied for crossover probability. According to adaptive probability, higher fitness individuals have lower probability for crossover. This means their good genetic information is preserved for the next generation. On the contrary, less-fitted solutions have a higher crossover rate and are more likely to be recombined in an effort to improve them. Adaptive probability P_c is defined in Equation 12:

$$P_c = \begin{cases} P_{c\_max} - \dfrac{\left(f' - f_{avg} \right)}{\left(f_{max} - f_{avg} \right)} \cdot \left(P_{c\_max} - P_{c\_min} \right) & f' > f_{avg} \\ P_{c\_max} & f' \leq f_{avg} \end{cases} \tag{12}$$

where

P_{c_max} and P_{c_min} = upper bound and lower bound for crossover probability, respectively;
f_{avg} = average fitness value of population;
f_{max} = maximum fitness value of population; and
f' = fitness value of given chromosome.

For the crossover operator, traditional two-point crossover is chosen. Everything between the two points is swapped between the parent chromosomes, rendering two child chromosomes.

Adaptive Mutation

Mutation prevents the search from being trapped in a local optimum point, by introducing new genes to the selected chromosome. The adaptive method is again used to decide the mutation prob-
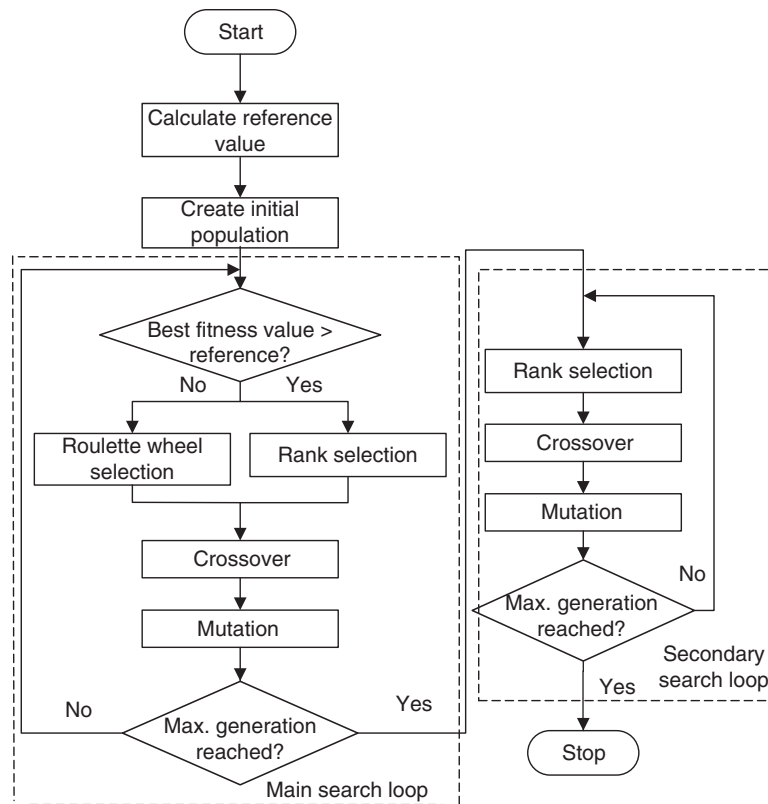
FIGURE 4 Enhanced GA procedure (max. = maximum).

ability for each chromosome. Similar to the crossover parameter, the actual mutation probability varies according to the fitness of the chromosome.

Proposed Algorithm Procedure

The proposed algorithm procedure is shown in Figure 4. In this procedure, a reference value will be calculated first. The reference value is the fitness value when both trains use the same single-train-based ATO control algorithm in opposite directions. It will be used as the threshold for the two selection methods in the main search loop later.

After creating an initial population, the search includes two steps: main search loop and secondary search loop. The main search loop tries to find the best-fitted individuals based on a randomly initialized population. Two selection methods are used to ensure population diversity during the early stage and efficient convergence during the later period. Once the main search loop ends, the best solution will be passed to the secondary search loop. A regular GA procedure is then followed to search the neighboring area around the best solution. The final optimal solution will be achieved after the two search loops are complete.

CASE STUDY

The study analyzed the simulation results that were obtained. Simulations were carried out on the basis of the platform developed by Visual C++ installed on a desktop computer with 8 GB of RAM

and a 3.2 GHz i3 processor, which allowed for verification of the effectiveness of the GAs on coordinated train control.

The chosen bidirectional simulation section is a part of the Xi'an metro line in China. The distance between the two selected stations is 4,977 ft, and the scheduled travel time is 115 s for both directions. Rated voltage for DC substations is 1,650 V. Internal resistance on the catenary is 43.45 mΩ/mi. The maximum train acceleration is 2.39 mph/s. Two trains were included in the simulation. The westbound train leaves the station 70 s later than the eastbound train.

A population of 60 randomly generated chromosomes with length 83 genes was used in the GA as the initial population. The maximum crossover rate is 0.8, while the minimum crossover rate is 0.4. The maximum mutation rate is 0.1, while the minimum mutation rate is 0.001.

To demonstrate the optimality of the coordinated control algorithm, the base case for the case study uses initial speed profiles developed for the eastbound and westbound trains with a single-train-based ATO algorithm (2). Therefore, their mechanical energy consumptions are already minimized; however, optimization of regenerative energy receptivity is not taken into account.

The case study was implemented in two steps. In the first step, with the above parameters, the optimized case where the westbound train applies the coordinated control algorithm with a synchronization time of 70 s was analyzed and compared with the base case. In the second step, scenarios with different synchronization times were developed to study the relationship between synchronization time and the optimization ratio.

The results of the first step of the case study are shown in Figure 5. The dash-dot line is the speed profile of the eastbound train. The
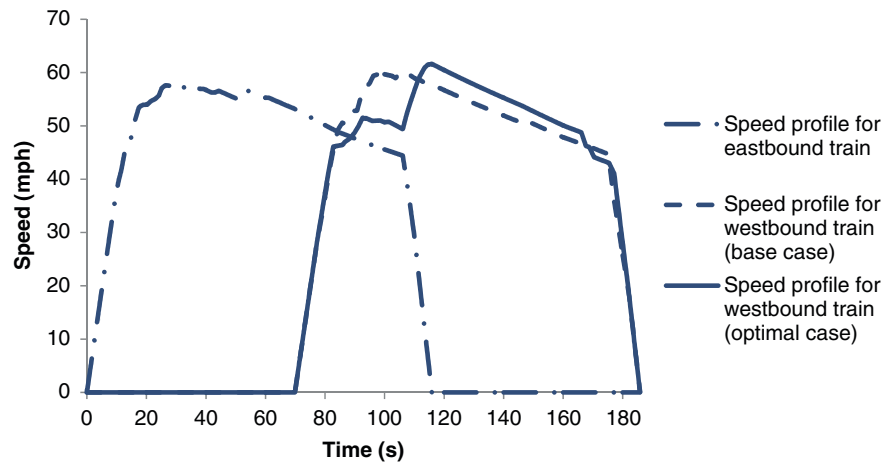
FIGURE 5   Simulation results: speed profiles.

dashed line is the speed profile of the westbound train in the base case. The solid line is the speed profile of the westbound train in the optimal case. The three speed profiles are plotted in the same time scale and the westbound train departs 70 s later than the eastbound train.

In the base case, the two trains are under the control of the single-train-based ATO algorithm. In the optimal case, the eastbound train is operated with the same original commands. The westbound train deviates from the original profile, adjusting its actual tractive and braking efforts according to the energy available on the catenary and to make use of the regenerative energy from the eastbound train. After the eastbound train stops, the westbound train mainly applies coasting and braking during the rest of the journey, avoiding additional energy consumption.

As shown by the simulation results in Table 1, regulating the speed of the westbound train according to the braking state of the eastbound train reduces total system energy consumption at the substation by 12.7%. The time and distance deviations are only 0.69% and 0.08%, respectively, from the required 115 s and 4,977 ft. For the daily 18 h operation of a metro transit system, assuming 6 min headway for 8 h, and 12 min headway for 12 h, application of the coordinated driving strategy could save 652.4 kW-h for an inter-station section per day. Furthermore, for a metro line with 15 stations, annual savings of $400,000 are estimated with the reduction in train operating cost.

Another benefit of speed coordination is reduced voltage fluctuation. Frequent voltage fluctuation will harm the onboard and sub-station electrical equipment, impacting system reliability. When a train accelerates and requires energy from a substation, the catenary voltage of the train will drop significantly. However, when part of the train's required traction energy can be fed from another train in regenerative braking, less energy is required from the power station, and the voltage drop is decreased. The voltage performance of the case study is illustrated in Figure 6.

For further investigation of the performance of the coordinated train control algorithm, the energy saving levels at different synchronization times, from 10 to 100 s, were tested.

Figure 7*a* shows the energy consumption for the base case and the optimized case for different synchronization times. Figure 7*b* shows the corresponding ratio of optimized to base energy consumption, which is called the energy optimization ratio. When both trains apply single-train-based ATO algorithms as in the base case, system energy consumption decreases as the synchronization time increases. Without optimization, energy consumption can be reduced by 18% by increasing synchronization time from 10 to 100 s. Through optimization and introducing regenerative energy recovery into the ATO algorithm, further reductions can be achieved for a given synchronization time. The benefit of optimization is relatively small when the synchronization time is near 10 or 100 s, while the optimization ratio reaches its peak (12.7%) at 70 s.

As shown in Figure 5, when the westbound train leaves the station 70 s after the departure of the eastbound train, the westbound train will start coasting at 100.1 s, waiting for regenerative energy to become available on the catenary for further acceleration. The longer the west-bound train coasts, the more time is lost. To satisfy running time constraints, the westbound train must accelerate longer to a higher speed to compensate for this time loss, offsetting some of the benefits from reuse of regenerative energy. As the synchronization time increases, the position of the westbound train during acceleration is closer to the regenerative braking point of the eastbound train, and it is easier for the westbound train to postpone acceleration without compromising the time constraint. As more regenerative energy is able to be absorbed, the benefits of optimization increase, as illustrated by the vertical distance between the two lines plotted in Figure 7*a*. However, at some particular synchronization time (100 s in this example), the eastbound train uses regenerative braking at the exact departure time of the westbound train, and the regenerative energy can be easily absorbed by simply applying maximum acceleration under the default speed profile. Since further speed profile optimization cannot improve on this scenario facilitated by coincidental timing of maximum acceleration and braking, the base and optimized energy consumption results converge at this point.

TABLE 1   Simulation Results for Westbound Train

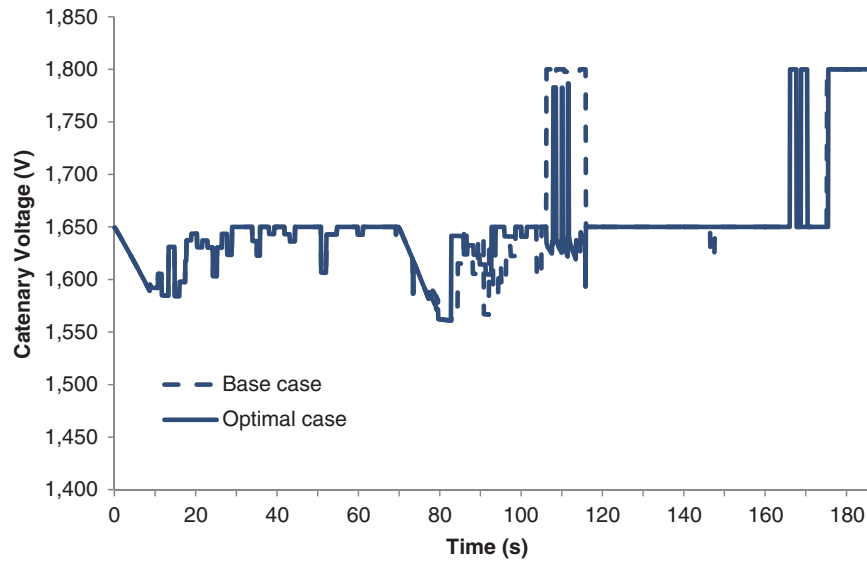| Case	System Energy (kW-h)	Time (s)	Distance (ft)
Base	36.69	115.9	4,970.76
Optimized	32.03	115.8	4,973.03

FIGURE 6   Simulation results: catenary voltage.

CONCLUSION

This study established a mathematical energy consumption model of bidirectional trains running in the same power section, based on train operation and electrical theories. GAs were applied to generate an optimal speed profile for the second train to minimize energy consumption at the power substations. Improvements like dual search loops and adaptive probability were introduced to the GA formulation to ensure the efficiency and effectiveness of the algorithm.

Although the energy savings from regenerative braking was estimated to be between 10% and 45% (*1*), this level usually cannot be reached because of various factors. Based on current system regenerative receptivity levels, the simulation results show that the coordinated train control algorithm can save up to 12.7% additional regenerative energy, enabling the system to receive more benefit from regenerative braking.

The investigation also showed that the optimization ratio from the coordinated train control algorithm differs according to the different synchronization times predefined by the timetable. Different synchronization times may have different optimization ratios.

The method proposed in this study can be used for multitrain-based ATO control algorithm design in DC traction power systems (valid for overhead catenary and third rail systems). The study of the optimization ratio for different synchronization times can be used to aid the design of energy-efficient timetables.

FUTURE WORK

The next step for model improvement will be to consider more interstation sections for optimization. When a power substation covers more than one interstation section, regenerative braking trains in one section can provide energy for accelerating trains in another section, providing more possibilities to improve regenerative energy receptivity and reduce power fluctuation. However, because of different electrical structures and power loss during transmission, the ATO control algorithm and corresponding optimization ratio may be different. Future study will allow the model to be improved so that it can better represent the actual conditions of metro transit systems and be applicable to a wider range of scenarios.
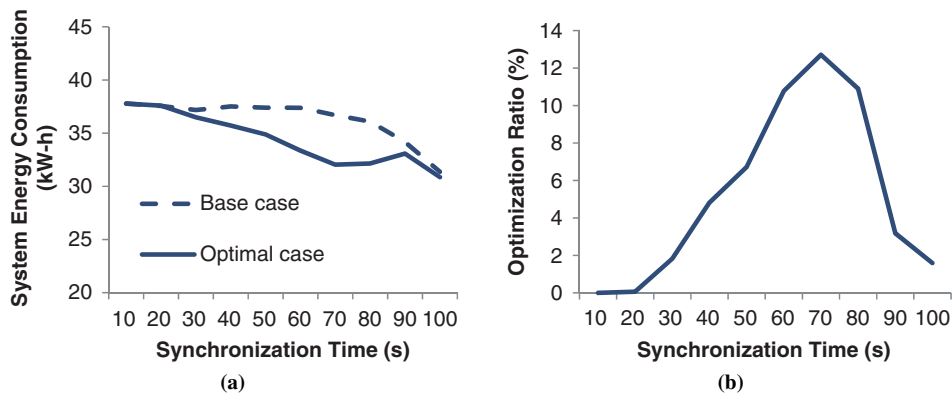

FIGURE 7   Energy evolutions at different synchronization times: (*a*) system energy consumption and (*b*) optimization ratio.

ACKNOWLEDGMENTS

REFERENCES

1. González-Gil, A., P. Roberto, and B. Paul. Sustainable Urban Rail Systems: Strategies and Technologies for Optimal Management of Regenerative Braking Energy. *Energy Conversion and Management,* Vol. 75, 2013, pp. 374–388.
2. Chang, C. S., Y. H. Phoa, W. Wang, and B. S. Thia. Economy/Regularity Fuzzy Logic Control of DC Railway Systems Using Event-Driven Approach. *Electric Power Application,* Vol. 143, No. 1, 1996, pp. 9–17.
3. Firpo, P., and S. Savio. Optimized Train Running Curve for Electrical Energy Saving in Autotransformer Supplied AC Railways. *Proc., IEEE Conference Electric Railways in a United Europe,* Amsterdam, Netherlands, IEEE, New York, 1995, pp. 23–27.
4. Gordon, S. P., and D. G. Lehrer. Coordinated Train Control and Energy Management Control Strategies. *Proc., ASME/IEEE Joint Rail Conference,* Philadelphia, Pa., IEEE, New York, 1998, pp. 165–176.
5. Albrecht, T. Reducing Power Peaks and Energy Consumption in Rail Transit Systems by Simultaneous Train Running Time Control. *Computers in Railways IX,* 2004, pp. 885–894.
6. Boizumeau, J., P. Leguay, and E. Navarro. Braking Energy Recovery at The Rennes Metro. *Workshop on Braking Energy Recovery Systems–Ticket to Kyoto Project.* Bielefeld, Germany, 2011.
7. Dingler, M. H., Y.-C. Lai, and C. P. L. Barkan. Effects of Communications-Based Train Control and Electronically Controlled Pneumatic Brakes on Railroad Capacity. In *Transportation Research Record: Journal of the Transportation Research Board, No. 2159,* Transportation Research Board of the National Academies, Washington, D.C., 2010, pp. 77–84.
8. Ichikawa, K. Application of Optimization Theory for Bounded State Variable Problems to the Operation of a Train. *Bulletin of Japanese Society of Mechanical Engineering,* Vol. 11, No. 47, 1968, pp. 857–865.
9. Howlett, P. G. The Optimal Control of a Train. *Annals of Operations Research,* Vol. 98, 2000, pp. 65–87.
10. Tang, H., J. Zhu, Q. Wang, and X. Feng. An On-Line Adjustable Control Algorithm for On-Time and Energy Saving Operations of Trains. *China Railway Science,* Vol. 34, 2013, pp. 90–95.
11. Yasunobu, S., S. Miyamoto, and H. Ihara. Fuzzy Control for Automatic Train Operation System. *Control in Transportation Systems* (D. Klamt and R. Lauber, eds.), A. Wheaton and Co., Exeter, United Kingdom, 1983, pp. 33–39.
12. Chang, C. S., and S. S. Sim. Optimizing Train Movements Through Coast Control Using Genetic Algorithms. *Electric Power Applications,* Vol. 144, No. 1, 1997, pp. 65–73.
13. Masafumi, M., and M. Kunihiko. Energy Saving Speed and Charge/Discharge Control of a Railway Vehicle with On-Board Energy Storage by Means of an Optimization Model. *IEEJ Transactions on Electrical and Electronic Engineering,* Vol. 4, No. 6, 2008, pp. 771–778.
14. Masafumi, M., and K. Hideyoshi. Optimization of Train Speed Profile for Minimum Energy Consumption. *IEEJ Transactions on Electrical and Electronic Engineering,* Vol. 5, No. 3, 2010, pp. 263–269.
15. Tang, H., Q. Wang, and C. T. Dick. Optimizing Train Speed Profiles to Improve Regeneration Efficiency of Transit Operations. *Proc., 2014 Joint Rail Conference,* Colorado Springs, Colo., American Society of Mechanical Engineers, Washington, D.C., 2014, pp. 1–9.
16. *IEEE Standard for Communication Based Train Control (CBTC) Performance and Functional Requirements,* IEEE Std. 1474.1, 1999, pp. 6–29.
17. Allen, J. G., J. P. Aurelius, and J. Black. Electric Power Supply for Commuter Rail: Are Railroads Keeping Up? In *Transportation Research Record: Journal of the Transportation Research Board, No. 2219,* Transportation Research Board of the National Academies, Washington, D.C., 2011, pp. 88–96.
18. Yu, J. G. Computer Modeling for Complex Engineering Decisions: Traction Power System Study for Metro-North Railroad. *International Conference on Computer Modeling for Rail Operations,* Delray Beach, Fla., 2004, pp. 2–19.

The Standing Committee on Rail Transit Systems peer-reviewed this paper.